



Behaviour of Light-Weight Ferrocement under Monotonic Axial Compression

Prakash K E¹, Shesha Prakash M N², Gangadharappa B M³ and Suresh G S⁴

Professor of Civil Engineering, Registrar, Visvesvaraya Technological University, Jnana Sangama, Belgaum-590018, Karnataka.

Vice Principal, Professor and Head of Civil Engineering, Vidya Vikas Institute of Engineering & Technology, Bannur Road, Mysore-570028, Karnataka

Professor of Civil Engineering, J.N.N. College of Engineering, Shimoga-577204, Karnataka

Professor of Civil Engineering, National Institute of Engineering, Mysore-570004, Karnataka

Abstract: *The main investigation in this research work is to maintain the eco-balance by preventing the open site dumping of the Blast furnace slag (BFS), a by-product in the process of cement production is an industrial waste, causing environmental pollution and prevention of sand mining by the replacement of Slag for fine aggregates in ferrocement. Sand mining has led to the danger of river-course change and causing floods. This replacement has been found to improve the strength characteristics of ferrocement and also makes it lightweight. This not only helps in construction of multi storied structures but also found to maintain thermal comfort.*

The main investigation is regarding the percentage replacement of sand by BFS and reinforcing with meshes. It is observed that the ultimate strength reaches a peak value and later decreases due to replacement of BFS. Marginal decrease in ultimate strength with increase in mesh content has also been observed. Further, with the cracks developed parallel to the mesh layers, the weak planes are generated along the mesh layer which has hastened the failure. The experimental results are analysed and a theoretical solution has been developed for the computation of stress corresponding to strain.

Keywords: *Cement, Blast Furnace Slag (BFS), Wire meshes, Lightweight Concrete, Ferrocement, Monotonic stresses, Cyclic stresses*

I. Introduction

BFS is defined by the American Society for Testing and Materials (ASTM) as the non-metallic product consisting essentially silicates and alumina-silicates of calcium and other bases that is developed in a molten condition simultaneously with iron in a blast furnace. If the cooling of the slag is done with excess of water, granulated slag is formed which is used in the manufacture of blast furnace slag cement. If cooling is done with a limited amount of water in such a way as to strip steam in mass, it produces a porous, honeycombed material, which resembles pumice. Sometimes, the molten slag is rapidly agitated with limited amount of water and the steam and gas produced are made to get entrapped in the mass. Such a product is also called foamed slag or expanded slag. The texture and strength of foamed slag depends upon the chemical composition and the method of production. In the recent times slag is being utilised to avoid Environmental pollution (industrial). Slag resembling a molten metal, comes from the furnace in the liquid form at about 1480° C. Slag can be classified as three distinct types, air-cooled, expanded or granulated, depending on the manner in which the molten slag is cooled and solidified. Expanded slag can be used as both fine and coarse aggregate in the manufacture of lightweight concrete for structural purposes, floor-fills, concrete products, and masonry units. Structural lightweight concrete made with expanded slag exhibits high strength, low unit weight, durability, low heat transmission, good bond, low creep, and is free from alkali reactivity. Slag concrete is excellent for precast and pre-stressed shapes because of its lightweight and high early compressive and flexural strength. The authors have under taken research work on the Study of BFS Ferrocement under monotonic and cyclic Loading. This paper presents some experimental results analysed with respect to BFS ferrocement specimens under monotonic compression loading.

II. Research Significance

Ferrocement is a thin reinforced matrix used as structural elements, cladding element etc., subjected to various loading conditions like cyclic loading due to earthquake, wind etc.

The lightweight ferrocement is useful in the construction of boats, roofing systems etc., The lightweight material reduces self weight of the structural element.

The results of this investigation, is used in predicting the behaviour of lightweight ferrocement under cyclic loading. The research of this type of loading is underway by the authors.

The results obtained in this research, is useful in predicting moment curvature relationship of lightweight ferrocement under flexural monotonic loading.

III. Literature Review

Considerable amount of research work has been done on normal ferrocement¹. Even though the investigations are reported on ferrocement, literature on lightweight ferrocement in which sand replacement by blast furnace slag has been found to be few.

Said Abid El-Fattah El-Kholy² has conducted compression tests on lightweight ferrocement using BFS on a prism size of 100 mm x 100mm in cross section and 200 mm in height and varying the number of wire mesh layers with different percentages of BFS. He has recommended that the ultimate compressive strength of the prisms increases with the increase of number of mesh layers for all replacement percentage of BFS used. Sand replacement by BFS reduces the ultimate strength of specimens for all wire mesh contents used. The reduction increases with the increase of replacement percentage.

Some studies have been done on lightweight aggregate concrete ACI Committee³, Yingqin “Elaine” Jin *et al.*⁴, Jin *et al.*⁵ conducted compression tests on specimens with substitution of fly ash, slag and chemical admixtures in concrete mix design. They concluded that the slump of fly ash and slag concrete varies significantly with the substitution of fly ash, air-entraining agent, and types A, D and G admixtures, compared to that of the original fly ash concrete mixtures. Air content of fly ash and slag concrete also varies significantly due to the substitution of fly ash, air entraining agent. Compressive strength in concrete with the substitution of fly ash, slag, air-entraining agent, and types A, D and G admixtures surpass the target compressive strength in almost all cases. It is recommended that the results from this study be considered as an initial and preliminary effort. The results obtained show that the substitution of fly ash, slag, types A, D and G admixtures cause variability in concrete properties such as air content and slump. They recommended that more extensive studies were required.

Desayi and Jacob⁶ conducted uni-axial compression test on solid and hollow ferrocement prisms. Based on their test results they proposed equations to relate the compressive strength of ferrocement specimens with the compressive strength of mortar cube through a parameter called mesh-mortar parameter. The proposed mesh-mortar parameter is a non-dimensional quantity and is equal to $P_m (f_s/f_{cu})$ in which P_m is the proportion of areas of mesh wires in the direction of loading, f_s is the ultimate tensile strength of mesh wires and f_{cu} is the 100 mm cube strength of mortar. They concluded that, with the increase of the percentage of steel wires, ultimate strength of ferrocement slightly increased, and the strain at the ultimate strength was also greater.

Pama *et al.*⁷ experimentally showed that the ultimate compressive strength of ferrocement is lower than that of an equivalent pure mortar. They assumed that the compressive strength of ferrocement at ultimate is $0.85 f_c$ where f_c is the ultimate compressive strength of mortar.

Johnston and Mattar⁸ conducted compression tests on prismatic ferrocement specimens using welded meshes and expanded wire meshes. The welded wire meshes were used in orientations where the wires are parallel and perpendicular to the direction of the applied stress (0/90) or 45 to it (45/45). They concluded that the lateral steel carries 17% - 42% of the total load and the longitudinal steel carries 5-14%. They reported that the rectangular mesh with the larger amount of steel deployed in the lateral direction should give better strength–cost effectiveness than square mesh.

Desayi and Joshi⁹ conducted compression tests on undulated ferrocement wall elements of 20 mm in thickness to determine the influence of slenderness ratio and the amount of reinforcement. They concluded that, there is no appreciable difference in the strength of ferrocement plates and plain mortar plates in the range of mesh quantity used in that study. They also concluded that the compressive strength of the plates, on an average can be taken as 83% of the strength 100 mm mortar cubes.

The ACI Committee¹⁰ also reported that as a first approximation, the nominal compressive resistance of ferrocement elements subjected to uni-axial compression can be derived from the load carrying capacity of the un-reinforced mortar (concrete) matrix assuming a uniform stress distribution of $0.85 f_c$, where f_c is the design compressive strength of the mortar matrix.

Rathish Kumar *et al.*¹¹ carried out an experimental investigation to know the stress–strain behavior of ferrocement confined reinforced concrete (FCRC) under axial compression by varying specific surface factor (S_f), which controls the behavior of ferrocement and confinement index (C_i), which controls the behavior of tie confinement. A total of 108 specimens of size 150 x 150 x 300 mm were tested. The results indicated that the additional confinement in the form of ferrocement shell has improved the ultimate strength, strain at ultimate strength and the ductility of high strength concrete. Prediction equations for ultimate strength, strain ultimate strength and ductility for high strength concrete confined with ferrocement shell in addition to ties are presented. A review of the literature reveals that, the amount of work that has been carried out on lightweight ferrocement till date is inadequate. In the present investigation the effect of replacing sand by blast furnace slag and the effect of wire mesh on the behaviour of lightweight ferrocement in compression has been examined

IV. Experimental Programme

A. Materials used

a. Cement: Ordinary Portland cement conforming to IS: 8112-1989, which was stored in a cool and dry place, was used. The physical properties of cement are as shown in table-1.

Table – 1

Properties of Cement	Values
Normal consistency (%)	37.5
Initial setting time (minutes)	40
Final setting time (minutes)	270
Fineness of cement (%)	95%
Specific gravity	2.53
Cube Compressive Strength: 3 Days (N/mm ²) 7 Days (N/mm ²)	21.54 22.87

Table – 2

Properties of Sand	Values
Fineness modulus	2.95
Density (kN/m ³)	1.54
Water content (%)	0.63
Specific gravity	2.41
Grading zone	III

b. Sand: River sand has been used as fine aggregate and the physical properties of sand are as shown in table - 2.

c. Blast furnace slag: The blast furnace slag Shown in Fig. 1 used to replace sand is mixed in different proportions in concrete. The physical properties and chemical composition of this lightweight aggregate given by the supplier are as shown in table - 3.



Fig. 1 - Lightweight B.F.S

Table - 3

Composition of BFS	% Present
SiO ₂	30-33
Al ₂ O ₃	20-22
CaO	33-35
MgO	09-10
S	Traces
Others	3-5
Fineness modulus	3.95
Density	1.12
Specific gravity	2.30
Grade Zone	I

d. Wire meshes: Galvanised woven square meshes of 4 x 20 gauge size 0.78 mm average wire diameter at 6.35 mm nominal spacing have been used as shown in Fig.2.

This tensile test was carried out in Universal strength testing machine, manufactured from Houns field – U.K. and the machine was fitted with data logger. The maximum loading capacity of the machine was 5000 N and the speed of the machine was 0.5 to 500 mm/minute. The experiment was conducted at the speed rate of 3 mm/minute as shown in Fig. 3. The ultimate tensile strength and the stress-strain plot of mesh wires are as shown in Fig. 4.

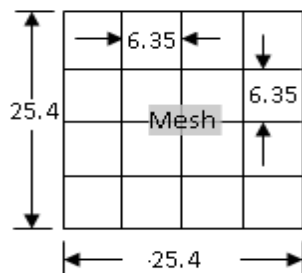


Fig. 2 - Details of Wire Mesh



Fig. 3 - Universal Strength Testing

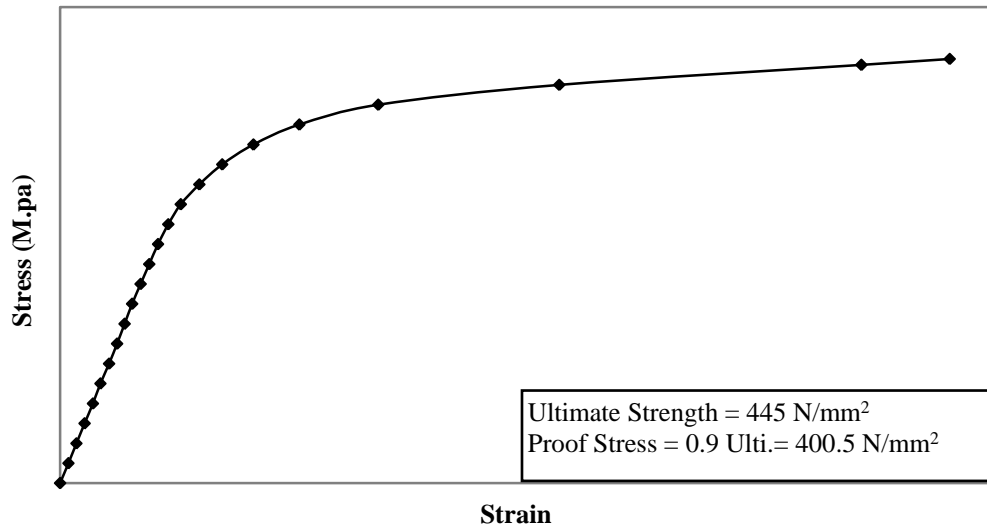


Fig. 4 - Stress-Strain Curve for 20 Gauge GI wire under monotonic loading

e. **Water:** Ordinary potable water was used.

V. Specimen preparation

Test specimens: The test specimens used in this study are prismatic in shape; the prism was 100 x 100 mm in cross-section and 200 mm long as shown in Fig. 5.

b) Casting of specimens: Mortar used in this investigation had a mix proportion of cement to sand as 1:2 by weight with water-cement ratio of 0.5. The proportion of mortar is used in this research work or (investigation) based on workability and cube strength of the mortar. While casting, the mesh layers were placed in the test specimen parallel to the direction of loading, i.e. parallel to the height of the specimen to simulate what usually happens in the practical applications of ferrocement in compression. Specimens and control cubes were cast as per standard norms¹⁷. In order to achieve uniform distribution for the wire mesh layers throughout the specimen thickness, suitable metallic spacers were used which were later removed. Compaction was done using table vibrator. The two parameters considered in this study are, the percentage of sand replacement viz., 0%, 20%, 35% and 70% by weight and volume fraction of mesh wires in terms of number of mesh layers per specimen viz., 0, 2, 4, 6 and 8 mesh layers

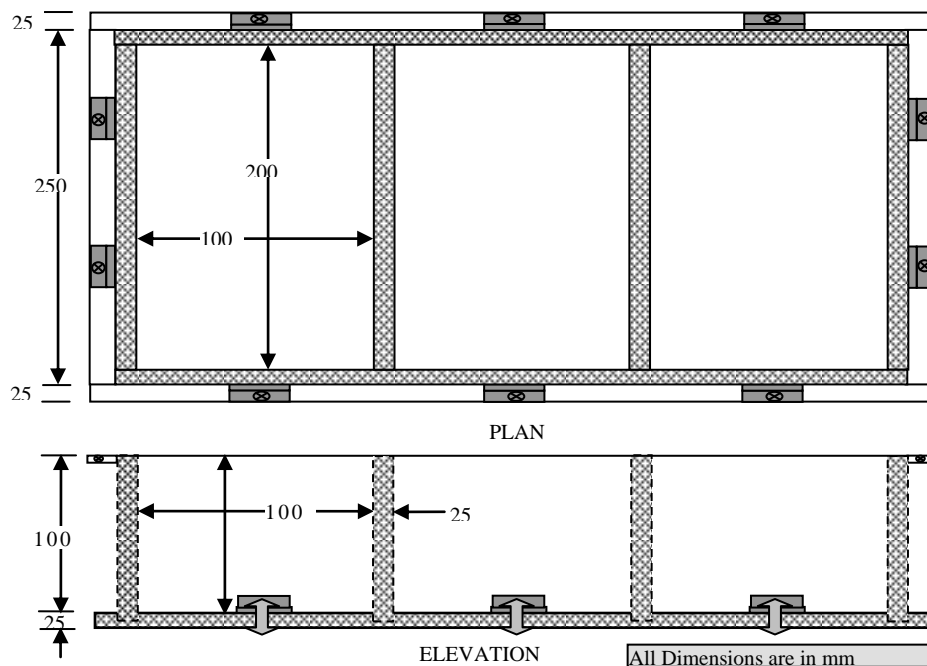


Fig. 5 - MOULD DETAILS

Table 4 - Designation of the specimens

No. of mesh layers	Percentage replacement of B.F.S. of 1:2 cement mortar			
	0	20	35	70
0	A0-0	A20-0	A35-0	A70-0
2	A0-2	A20-2	A35-2	A70-2
4	A0-4	A20-4	A35-4	A70-4
6	A0-6	A20-6	A35-6	A70-6
8	A0-8	A20-8	A35-8	A70-8

The different combinations of these parameters resulted in 20 groups of specimens as given in table 4. In each group three specimens were cast and tested (total of 60 specimens). The specimens were designated as A_{ij} , where i indicate percentage replacement of sand with BFS and j indicates number of mesh layers.

Testing of specimens:

Static axial compression load was applied gradually to the specimen using Universal Testing Machine (UTM) and deformation for each increment of load was measured using compresso-meter. Arrangement for the measurement of the axial deformation over the central length of 100 mm of the specimen is shown in the Figs. 6, 7 and 8. This arrangement consists of four dial gauges fitted at four diametrically opposite points between two square frames, which is attached to the test specimen. The whole assembly of specimen with the square frames was held in between the plates of a UTM. The compresso-meter was removed from the specimen after the load reached 50% of anticipated ultimate load and the loading was continued until the failure of the specimen.

The deformations were measured on all the four sides of the specimen, the average of all the four readings at each stage of loading was taken to represent the deformation between the gauge points of the specimen. Crack pattern of the specimens tested in compression are shown in Fig.9 ultimate strength of specimens and control cubes are given in Table 5.

Table 5 - Experimental Values of (BFS) Ferrocement

Designation of mix	% BFS	Mesh Layer	Comp Stress of Specimen (σ_u) (N/mm ²)	Cube Compressive Stress (σ_{cu}) (N/mm ²)	Normalization = $\frac{\sigma_u}{\sqrt{\sigma_{cu}}}$	% change of norm. w.r.t. 0% of BFS
1	2	3	4	5	6	7
A ₀₋₀	0	0	38.00	42.32	0.8979	-
A ₀₋₂		2	39.75	47.11	0.8438	-
A ₀₋₄		4	37.50	47.71	0.7861	-
A ₀₋₆		6	32.00	46.80	0.6838	-
A ₀₋₈		8	27.50	41.01	0.6705	-
A ₂₀₋₀	20	0	41.50	41.52	0.9995	11.31
A ₂₀₋₂		2	38.50	41.04	0.9381	11.17
A ₂₀₋₄		4	35.50	39.60	0.8965	14.04
A ₂₀₋₆		6	32.75	39.80	0.8229	20.34
A ₂₀₋₈		8	28.50	40.00	0.7125	6.26
A ₃₅₋₀	35	0	27.50	32.27	0.8523	-5.08
A ₃₅₋₂		2	27.00	34.13	0.7910	-6.26
A ₃₅₋₄		4	29.50	39.64	0.7442	-5.33
A ₃₅₋₆		6	30.75	46.59	0.6601	-3.46
A ₃₅₋₈		8	33.50	52.16	0.6423	-4.21
A ₇₀₋₀	70	0	31.50	39.84	0.7907	-11.95
A ₇₀₋₂		2	27.50	36.80	0.7473	-11.44
A ₇₀₋₄		4	31.00	44.00	0.7045	-10.37
A ₇₀₋₆		6	25.50	40.48	0.6299	-7.87
A ₇₀₋₈		8	24.50	41.52	0.5901	-11.99

VI. Results and discussions:

Mode of Failure and Cracking of Specimens

While testing, plain specimens (without mesh) failed suddenly on a diagonal plane at the appearance of the first crack. In specimens with wire meshes, the first crack always appeared vertically (parallel to the loading direction) and mostly along one of the mesh layers. After the appearance of first crack, the other cracks that formed also were almost vertical. With increase in the applied load, the vertical cracks increased in the diagonal direction and ultimately most of the specimens failed on a diagonal plane (Fig 9). In case of most of the specimens reinforced only with wire meshes, the external wire mesh layers showed tendency to buckle and cause spalling of mortar cover as shown in Fig 9. A typical plot of stress-strain curves is as shown in Fig.10 & 11.

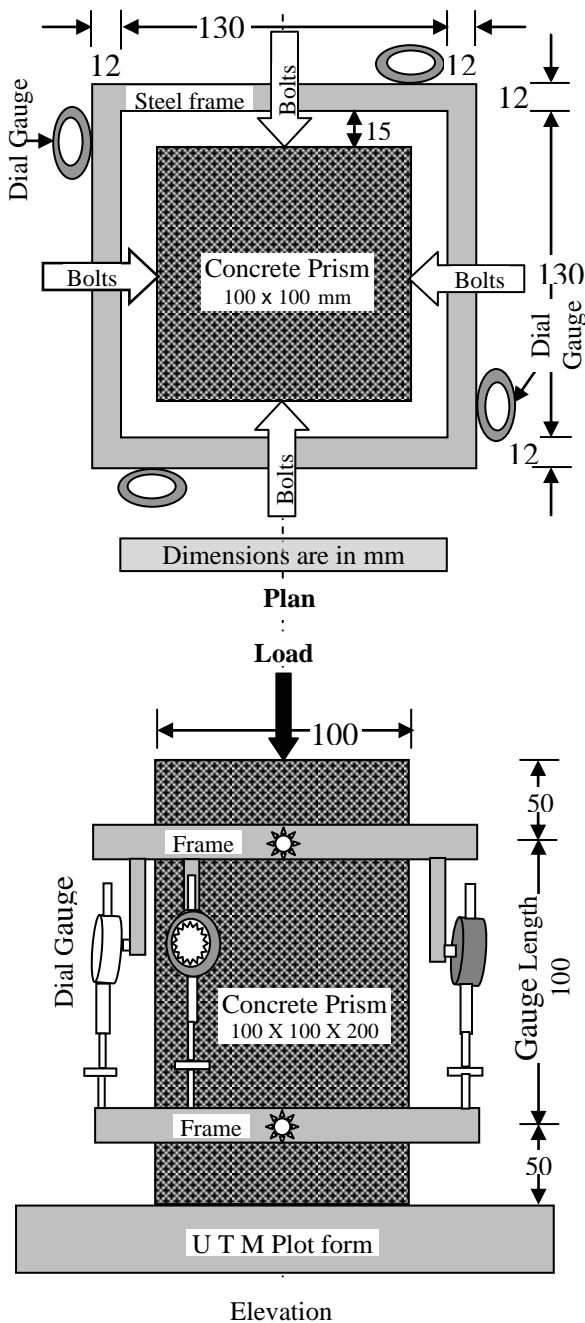


Fig. 6 – Compresso-meter

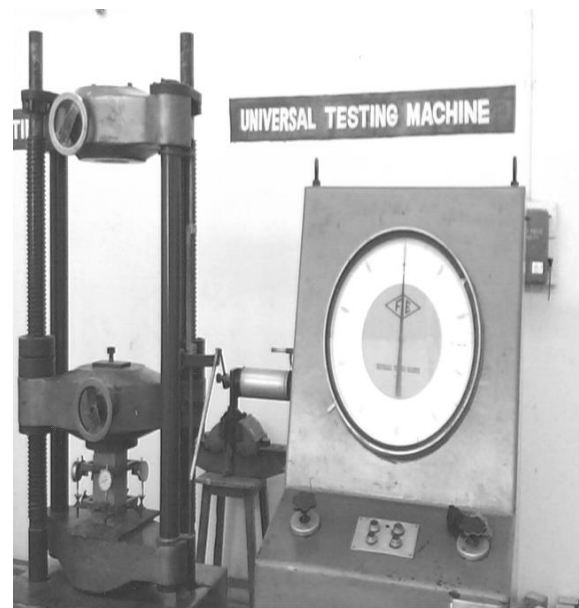


Fig. 7 - Testing of Specimen

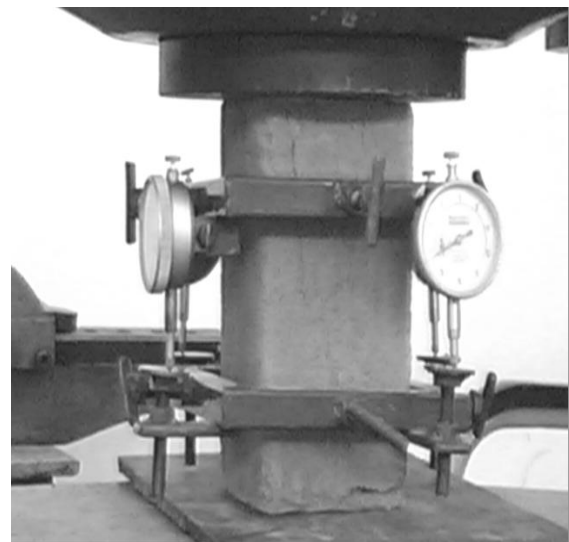


Fig. 8 Testing arrangements

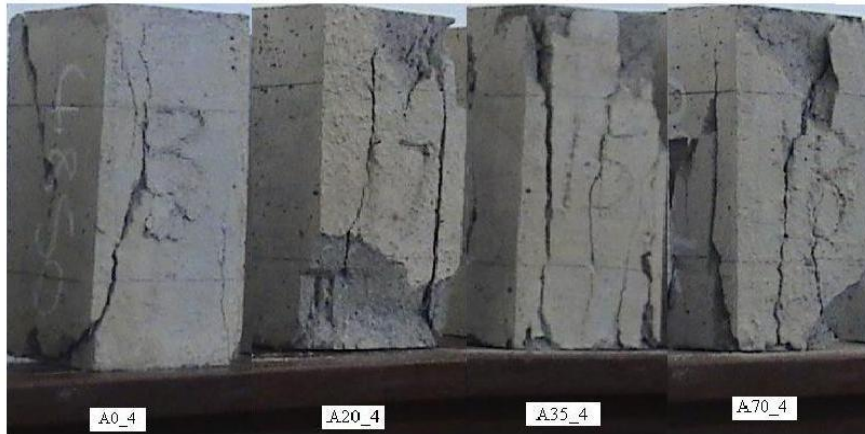


Fig. 9 - Typical Photos showing Cracking Pattern

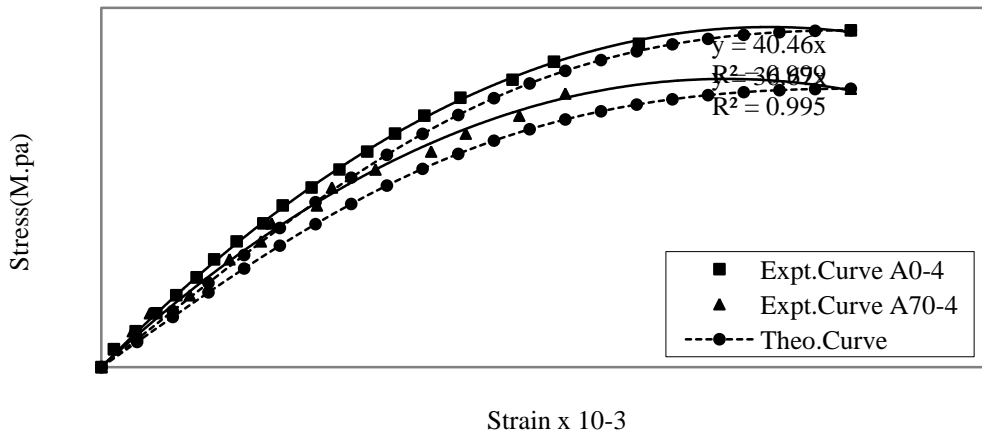


Fig. 10 - Experimental and Theoretical Stress - Strain Curves

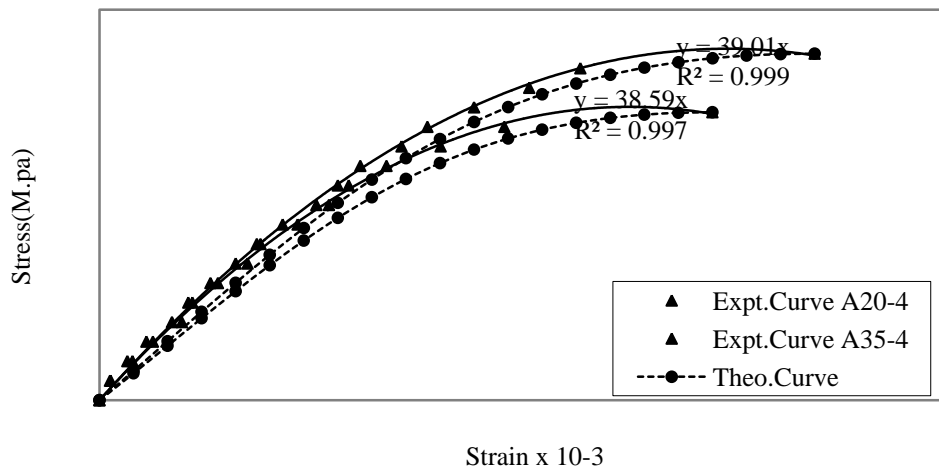


Fig. 11 - Experimental and Theoretical Stress - Strain Curves

Effect of BFS:

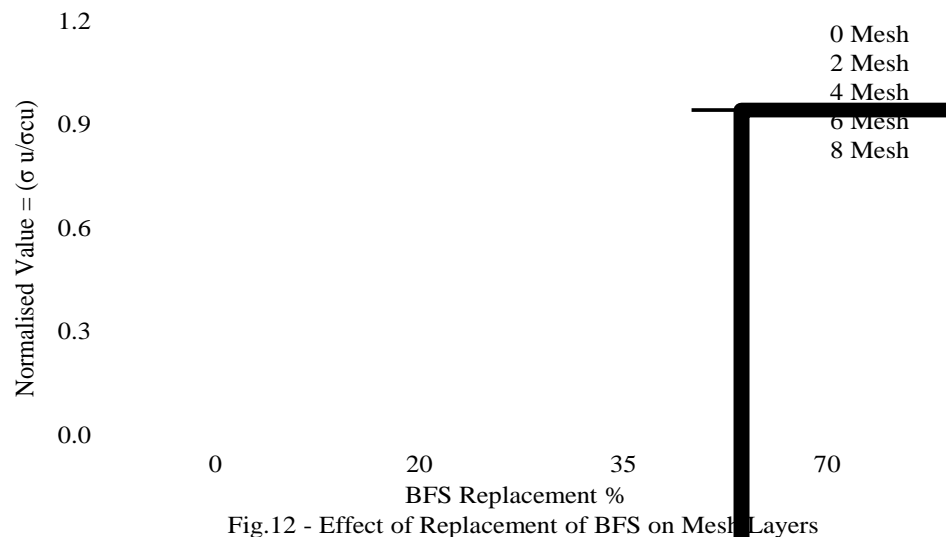


Fig.12 - Effect of Replacement of BFS on Mesh Layers

The effect of sand replacement by BFS on ultimate strength is shown in Fig.12 for all wire mesh contents used in this investigation. It is evident from Fig. that there is marginal increase in strength due to replacement of sand by BFS for all volume fractions of steel meshes which can be ignored. The use of natural sand being overexploited and is becoming extinct, use of BFS as a replacement to sand can avoid the environmental hazard and the weight of the structure can also be reduced. This reduction of weight improves the earthquake resistance of the structure.

Effect of mesh content on ultimate strength

Normalised ultimate strength shown in Fig.13 indicates that, the increase in mesh content does not increase the ultimate strength, but there is marginal decrease in ultimate strength with increase in mesh content. This may be due to buckling of small diameter of wires used in the mesh. This effect is observed in all the specimens with different percentage of replacement of sand by BFS.

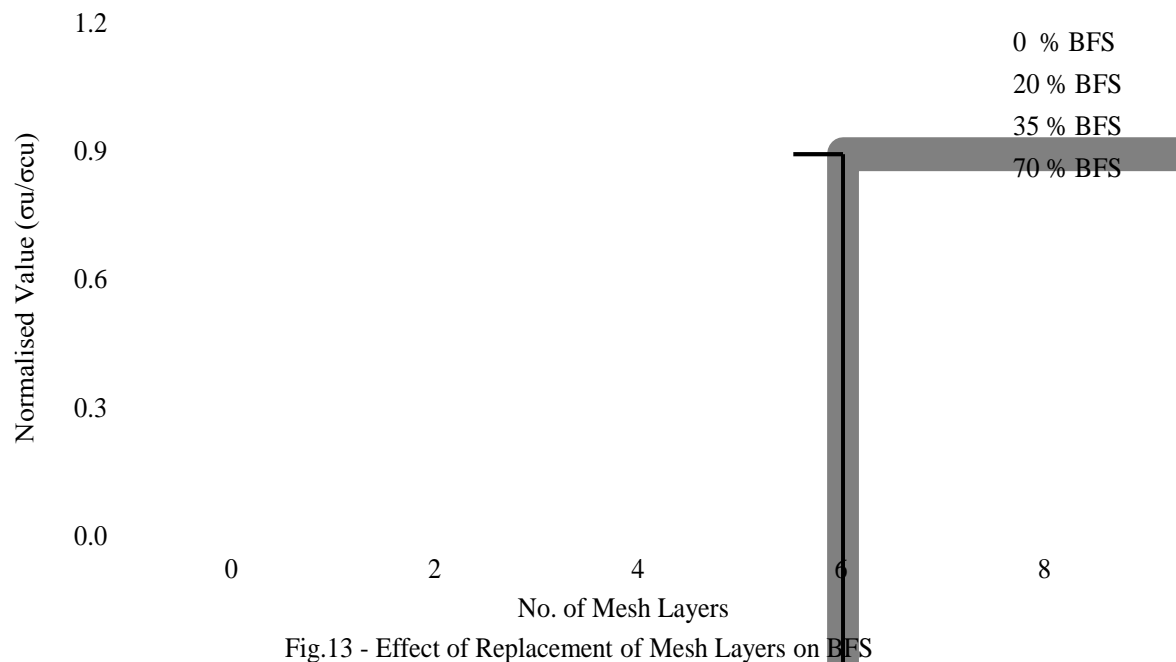


Fig.13 - Effect of Replacement of Mesh Layers on BFS

Theoretical Solution:

Proposed stress-strain equation

The general shape of the stress-strain diagram for ferrocement is similar to reinforced concrete (Logan and Shah)¹². It is clear from earlier reported investigations that, both the strength and deformation of concrete increases with the reinforcement, the increase in deformation being much greater than the increase in strength (Sanjeev Reddy)¹³. The steel resists the propagation of internal cracking and the deviation of the stress-strain curve from the initial straight-line portion takes higher stress. Suresh concluded that the proposed equation for concrete (Desayi)¹⁶ also holds good for ferrocement (Suresh)¹⁴. However, there is no reported work on lightweight ferrocement and hence an attempt has been made by the authors to develop a theoretical equation for the lightweight ferrocement.

Stress-Strain Equation:

It has been found that an equation of the type shown below for the confined reinforced concrete¹³ agrees fairly well for the ascending portion of the stress- strain curve in compression for Normal and Lightweight ferrocement.

$$\sigma = \frac{A\varepsilon}{1 + B\varepsilon + C\varepsilon^2 + D\varepsilon^3} \quad (1)$$

Where, σ and ε are the compressive stress and strains and A, B, C and D are the parameters to be obtained from the boundary conditions and the test results.

This equation is similar to the one suggested by Saenz¹⁵ for plain concrete, during his discussion on a paper by Desayi and Krishnan¹⁶. Referring to Fig.14, the conditions to be fulfilled by the stress-strain equation are:

As there is no descending curve in stress-strain graph in this investigation, the term D is omitted, so the equation is,

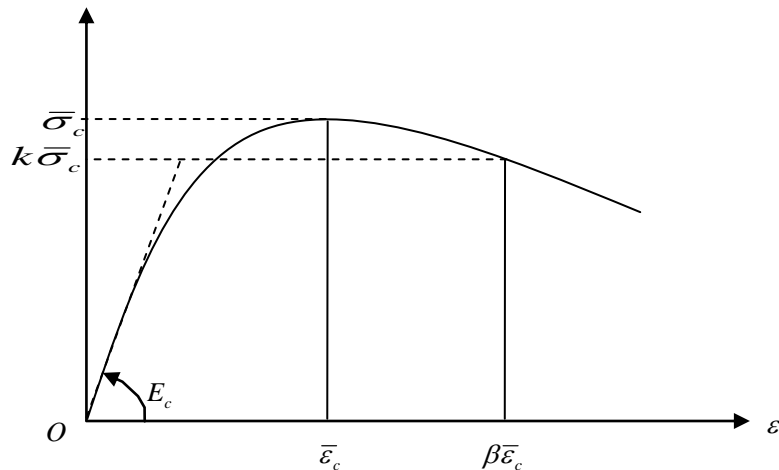


Fig.14 - Notation for proposed equation of stress-strain curve of Ferrocement

$$\sigma = \frac{A\varepsilon}{1 + B\varepsilon + C\varepsilon^2} \quad \text{-----} \quad (2)$$

Fulfilling these boundary conditions,

At $\varepsilon = 0; \sigma = 0$ & $\frac{d\sigma}{d\varepsilon} = E_c$ at the origin of the curve,

At $\varepsilon = \varepsilon_c; \sigma = \bar{\sigma}_c$ & $\frac{d\sigma}{d\varepsilon} = 0$ at the point of peak stress,

Differentiating w.r.to ε of equation 2

$$\frac{d\sigma}{d\varepsilon} = \frac{(1 + B\varepsilon + C\varepsilon^2)A - A\varepsilon(B + 2C\varepsilon)}{(1 + B\varepsilon + C\varepsilon^2)^2}$$

At $\varepsilon = 0; \frac{d\sigma}{d\varepsilon} = E_c$

$$E_c = \frac{(1 + 0 + 0)A - 0}{1}$$

Hence $A = E_c$

B.C. No. ii $\varepsilon = \bar{\varepsilon}_c, \sigma = \bar{\sigma}_c$ & $\frac{d\sigma}{d\varepsilon} = 0$

$$\bar{\sigma}_c = \frac{E_c \bar{\varepsilon}_c}{1 + B\bar{\varepsilon}_c + C\bar{\varepsilon}_c^2} \quad \text{-----} \quad (3)$$

Differentiating .w.r.to ε

$$\frac{d\sigma}{d\varepsilon} = \frac{(1+B\bar{\varepsilon}_c + C\bar{\varepsilon}_c^2)E_c - E_c\bar{\varepsilon}_c(B+2C\bar{\varepsilon}_c)}{(1+B\bar{\varepsilon}_c + C\bar{\varepsilon}_c^2)^2} \Rightarrow 0$$

$$(1+B\bar{\varepsilon}_c + C\bar{\varepsilon}_c^2)E_c = E_c\bar{\varepsilon}_c(B+2C\bar{\varepsilon}_c)$$

$$(1+B\bar{\varepsilon}_c + C\bar{\varepsilon}_c^2) = (B\bar{\varepsilon}_c + 2C\bar{\varepsilon}_c^2)$$

$$2C\bar{\varepsilon}_c^2 - C\bar{\varepsilon}_c^2 = 1$$

There fore $C\bar{\varepsilon}_c^2 = 1$

$$C = \frac{1}{\bar{\varepsilon}_c^2}$$

From equation 3

$$\frac{\bar{\sigma}_c}{E_c} = \frac{\bar{\varepsilon}_c}{1+B\bar{\varepsilon}_c + C\bar{\varepsilon}_c^2}$$

$$(1+B\bar{\varepsilon}_c + C\bar{\varepsilon}_c^2) = E_c \frac{\bar{\varepsilon}_c}{\bar{\sigma}_c} = \frac{E_c}{E'_c}$$

$$B\bar{\varepsilon}_c = \frac{E_c}{E'_c} - (1+C\bar{\varepsilon}_c^2) \quad \text{Substituting for } C$$

$$B\bar{\varepsilon}_c = \frac{E_c}{E'_c} - 2$$

$$B = \frac{1}{\bar{\varepsilon}_c} \left(\frac{E_c}{E'_c} - 2 \right)$$

The values of the parameters are:

$$A = E_c$$

$$B = \frac{1}{\bar{\varepsilon}_c} \left(\frac{E_c}{E'_c} - 2 \right)$$

$$C = \frac{1}{\bar{\varepsilon}_c^2}$$

Where,

$$E_c = \text{Initial tangent modulus of concrete} = 5000 * \sqrt{f_{ck}}$$

$$E'_c = \frac{\bar{\sigma}_c}{\bar{\varepsilon}_c} = \text{Secant modulus at the point of peak stress.}$$

For the Lightweight ferrocement, the constants evaluated from the boundary conditions and experimental results are:

Substituting for the parameters A, B & C the stress-strain equation will be

$$\sigma = \frac{E_c \varepsilon}{1 + \frac{1}{\bar{\varepsilon}_c} \left(\frac{E_c}{E'_c} - 2 \right) \varepsilon + \left(\frac{1}{\bar{\varepsilon}_c^2} \right) \varepsilon^2} \quad \text{----- (4)}$$

The graph shows (7 & 8) the experimental and theoretical stress-strain curve by using the above equation (4) for various replacements of BFS for specimens with 4 meshes.

VII. Conclusions

Following conclusions are drawn from this investigation.

Replacement of BFS helps in reducing weight of the structure and thus improving its earthquake resistance. Use of BFS also avoids environmental hazards due to open dumping of BFS and overuse of natural sand which has led to serious problems at the river beds and delta regions. It also improves the thermal comfort in the building. Marginal decrease in ultimate strength with increase in mesh content has been observed and this may be due to buckling of small diameter wires of the mesh. Further, the loss of volume of material in cement and slag in place of mesh layers may have also contributed to early failure. In addition, the weak planes are generated along the mesh layer (as the loading is done parallel to the mesh layer) might have hastened the failure as can be seen from the cracks developed parallel to the mesh layers.

The proposed stress-strain equation (Eq. 4) has been found to agree with all the experimental curves for lightweight ferrocement for all replacements of BFS and different number of mesh layers.

It is also found that the proposed stress-strain equation concur with the equations proposed by Desayi⁶ for confined concrete with slight modifications of the constants.

Detailed investigation required on the influence of chemicals and buckling of wires on ultimate strength is beyond the scope of this paper.

REFERENCES

- [1]. SURYAKUMAR, G.V., NARAYANASWAMY, V.P., AND SHARMA, P.C., Ferrocement- a Survey of Experimental Investigations, ACI Journal of Structural Engineering, Vol. 1, No.4, January 1974, pp 167-182.
- [2]. SAID ABD EL-FATTAH EL-KHOLY "Studies on Lightweight Fibrous ferrocement in compression, Tension and Flexure" a thesis Submitted for the Degree of Ph.D. Thesis in Indian Institute of Science, Bangalore-January 1990.
- [3]. ACI COMMITTEE, 304, "Batching, Mixing and Job control of Lightweight concrete", concrete International, vol.4, No.9, Sept. 1982, pp. 88-96.
- [4]. YINGQIN "ELAINE" JIN AND NUR YAZDANI, "Substitution of fly ash, slag, and chemical admixtures in concrete mix design" Journal of materials in Civil Engg. @ ASCE/ Nov/Dec-2003. pp 602- 608.
- [5]. JIN and YAZDANI, "Substitution of fly ash, and chemical admixtures in concrete mix design" Journal of materials in Civil Engineering @ ASCE/ Nov/Dec - 2003 pp.602-608.
- [6]. DESAYI P. and JACOB A.K., "Ferrocement-its Strength and behaviour in Compression", National Seminar on Materials and Technology, Madras, India, Feb.1973.
- [7]. PAMA. R.P., SUTHARATANACHAIYAPORN.C. and LEE.S.L., "Rigidities and strength of ferrocement", First Australian Conference on Engineering Materials, The University of New South Wales, 1974.
- [8]. JOHNSTON. C.D. and MATTAR.S.G. "Ferrocement - Behaviour in tension and compression", Journal of the Structural Division ASCE, May 1976, Vol.102, ST5, pp. 875-889.
- [9]. DESAYI. P. and JOSHI. A. D. "Ferrocement Load-bearing wall elements", Journal of the Structural Division, Proceedings of the American Society of Civil Engineers, Vol.102, No.ST9, September 1976 pp 1903-1916.
- [10]. ACI COMMITTEE, 549, "Guide for the Design, Construction and Repair of Ferrocement", American Concrete Institute Structural Journal, Vol.85, No.3, May-June 1988, pp 325-351.
- [11]. P.RATHISH KUMAR G. RAJESH KUMAR AND RAO A.K. "Ferrocement - An effective way of confining high strength concrete" Journal of Ferrocement Vol.35, No.1 January -2005 pp 514-525.
- [12]. LOGAN, D and SHAH, S.P. "Moment capacity and cracking behaviour of ferrocement in flexure", Journal of the American concrete Institute, Vol. 70, No. 12, December 1973, pp. 799- 804.
- [13]. SANJEEV REDDY, T. "Confined concrete and reinforced concrete members under monotonic repeated and reversed loading" Ph.D thesis, Indian Institute of Science, Bangalore-1977 pp 345-359, 412-431.
- [14]. SURESH G.S. "Studies on Ferrocement under monotonic, cyclic and repeated loading", Ph.D thesis, Indian Institute of Science, Bangalore, August 1995.
- [15]. SAENZ, L. P., DISCUSSION of a paper BY DESAYI, P., and S.KRISHNAN, Equation for the Stress-Strain Curve of Concrete, ACI Journal, Proceedings, Vol. 61, No. 9, September 1964 pp 1229-1235.
- [16]. DESAI, P., and KRISHNAN, S., Equation for the Stress-Strain Curve of Concrete, ACI Journal Proceedings Vol. 61, No. 3, March 1964 pp 345-350.
- [17]. INDIAN STANDARD INSTITUTION "Handbook on Concrete Mixes", based on Indian Standards, SP: 23 (S & T) - 1982 pp 23-24.

ACKNOWLEDGEMENT

The authors of the paper are grateful to the Managements and Principals of their respective institutes.